Study of the flat to slant crack transition in ductile thin sheet material: Simulations and experiments

T.F. Morgeneyer[1*], H. Proudhon[1], J. Besson[1]

[1] Mines ParisTech, Centre des matériaux, CNRS UMR 7633, BP87 91003 Evry Cedex, France

[*]thilo.morgeneyer@mines-paristech.fr

Flat to slant crack transition can typically be observed in ductile thin sheet materials. The crack initiates perpendicularly to the loading direction from the notch and then turns to 45° with respect to the loading direction during crack propagation. This phenomenon is, however, still not well understood and, so far, attempts to simulate the transition in three dimensions often fail to predict macroscopic loads correctly. In this study an initial attempt has been made to reproduce the flat to slant transition performing an implicit 3D Finite Element simulation via adapting a Gurson-type model. A second void nucleation term for deformation under shear was introduced. The Lode parameter was used here to identify shear deformation. Using this modification the flat to slant transition has been reproduced successfully at loads similar to the experimental results. Further experimental investigations of void growth in the flat and slant crack propagation regime have been carried out. Cracks in Kahn tear test specimens have been arrested in the three regimes and subsequently been observed via Synchrotron Radiation Tomography of the crack tips 3D quantitative void growth analyses ahead of the crack tip in the flat and slant regimes have confirmed the change in fracture mechanisms: void growth in the flat region is substantially higher as compared to the slant crack propagation region.

Keywords: flat fracture, slant fracture, Lode parameter, void growth, X-ray tomography

INTRODUCTION

In ductile fracture of sheet material, fracture initiation at the notch or precrack root typically commences with the formation of a flat triangular region (i.e., the normal to the crack corresponds to the loading direction). In this area, large primary dimples are observed. Once the initial triangle is formed, the crack tilts and becomes slanted forming approximately an angle of 45° with the loading direction. In this area, primary dimples are observed together with secondary dimples. Near the notch root of severely notched samples, the mean stress is higher which promotes void growth [1]. Experimental results indicate that in the slant fracture region, fracture is not dominated by void growth but by shear decohesion mechanisms [2, 3] or fracture on grain boundaries [4].

In a finite element study [5], the crack propagation of both a meshed flat and a slant crack have been investigated. The stress fields ahead of the respective cracks during crack propagation under remote mode I loading have been compared and it was identified that for a slant crack the constraint and the mean stress ahead of the crack are reduced whilst the effective stress is augmented compared to a flat crack. This promotes a shearing type of fracture.

Modelling of the flat to slant fracture transition is hard to perform and the fracture path is often only reproduced as flat fracture [1, 6]. Attempts have been made to reproduce the flat to slant fracture transition [7, 8, 9] but the fracture path and the macroscopic load could not be reproduced simultaneously. Often a comparison with experimental results is missing in the literature. Recent models try to extend the Gurson model, which correctly describes void growth at high levels of stress triaxiality, to cases of fracture at low levels of stress triaxiality.

The Lode parameter is often used to identify the occurrence of shear [9, 10] and will also be used in the present study.

MATERIALS AND TESTING

AA2139 sheet was supplied by Alcan CRV with a thickness of 3.2mm in a commercial T351 condition, *i.e.* solution treated, stretched and naturally aged. The composition ranges are given in Tab 1.

Si	Fe	Cu	Mn	Mg	Ag	Ti	Zn
<= 0.1	<= 0.15	4.5 - 5.5	0.20 - 0.6	0.20 - 0.8	0.15 - 0.6	<= 0.15	<=0.25

Table 1 : Composition limits of alloy AA2139 in weight %

Two orientations of loading in the sheet plane have been investigated for all samples: rolling direction (L) and long transverse direction (T). In Kahn samples loaded in the L direction, cracks will propagate in the T direction; these tests are referred to as L-T, and vice versa for T-L designated tests. Testing speeds and the sample geometry are given in [1]. More mechanical testing results and microstructural observations of this material may be found in [11, 6]

For Synchrotron Radiation Computed Tomography (SRCT) observations 3 different L-T Kahn tear tests [ASTM-international, Standard B 871 - 01. 2001] have been arrested at different loads : *i.e.* tests were arrested before final failure of the coupon. Arrows in Fig 1 indicate the loads at which the tests have been arrested.

To facilitate high resolution SRCT imaging of the arrested crack tip region, a small ‘stick’ of material (dimensions 1mm x 1mm x 10mm) was extracted around the tip at the specimen mid-plane (long dimension parallel to the direction of crack extension) using a slow speed diamond saw,

SRC Tomography was performed at beamline ID 19 of the European Synchrotron Radiation Facility (ESRF), Grenoble, France, at 20.5kV. In the reconstructed slices an isotropic voxel size of 0.7µm was obtained. Phase contrast imaging has been performed to enhance the detection of edges [12].

For the analysis of arrested cracks, use was made of custom image data manipulation routines. The cracks are first binarized using a series of morphological operations then analyzed using a ‘sum along ray algorithm’ [13]. The aim was to precisely determine and quantify the local crack characteristics such as opening within the 3D volume.

To quantify the damage ahead of the crack, the volume has been divided into cubes of 50µm edge length. The total analyzed volume was ~700 µm, 900 µm, and 500 µm in crack growth direction, crack width direction and direction normal to the crack respectively. The average void volume fraction in each cube has been determined. Subsequently one cube containing the maximum value in one column, (in the former loading direction) has been determined. These cubes containing the maximum void volume fraction have been retained and are displayed in the figures.

EXPERIMENTAL RESULTS

Mechanical Testing

Fig. 1 shows the experimental results of the Kahn tear testing for T-L and L-T orientations. The L-T configuration is tougher than the T-L configuration. Tests for SRCT observations have been arrested at points 1.,2. and 3. to capture the states of: 1.crack initiation, 2. flat to slant transition and 3. slant fracture.

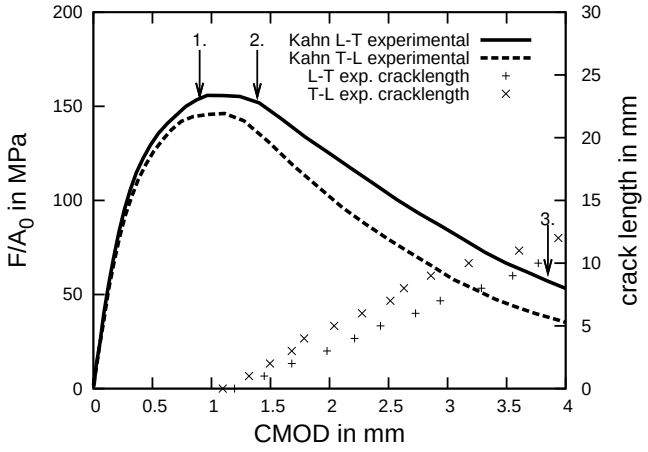

Fig. 1: Kahn tear test results for T-L and L-T testing orientations. Arrows indicate the 3 different points where tests have been arrested for tomography observation

Tomography

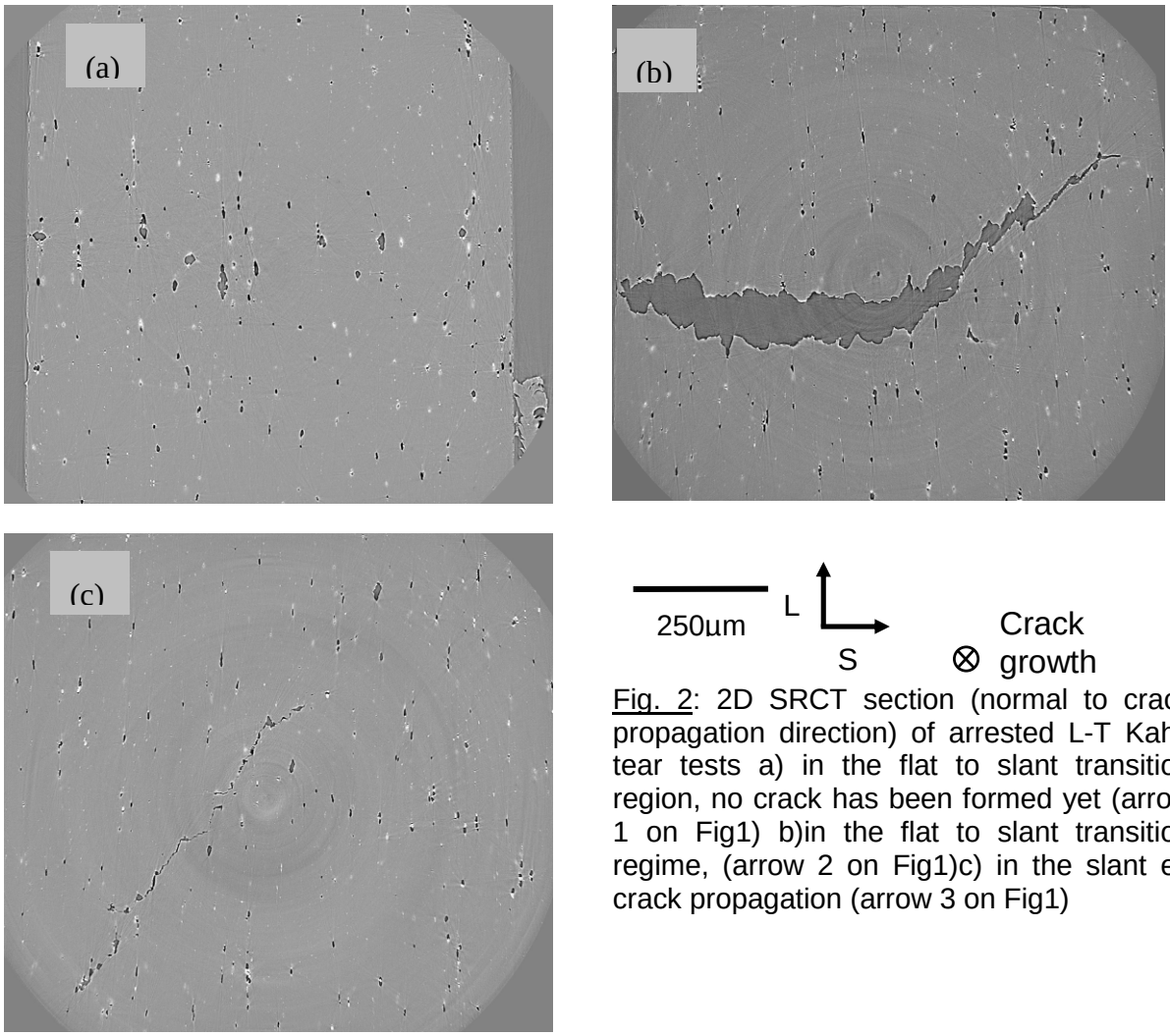

Fig. 2: 2D SRCT section (normal to crack propagation direction) of arrested L-T Kahn tear tests a) in the flat to slant transition region, no crack has been formed yet (arrow 1 on Fig1) b)in the flat to slant transition regime, (arrow 2 on Fig1)c) in the slant ed crack propagation (arrow 3 on Fig1)

Fig. 2 shows 2D sections of SRCT data with the crack propagation direction normal to the image plane. It can clearly been seen that for crack interruption at crack initiation (arrow 1 in Fig1) no macroscopic crack has formed but substantial void growth has taken place ahead of the machined notch (see Fig2(a)). For crack interruption in the flat to slant crack transition regime (arrow 2 in Fig 1, Fig 2(b)) the flat crack, oriented normal to the former loading direction, is wide open and substantial void growth has taken place. However in the slanted area of the crack only very limited void growth can be seen. The limited void growth and narrow crack opening is even more pronounced for the arrested crack in the propagation region. The observations of decreasing void growth are consistent with the decrease in stress triaxiality that takes place after crack initiation [1].
Fig 3(a) shows the analysis of an arrested crack in the fracture initiation regime where no crack has formed yet but substantial void growth has taken place ahead of the machined notch and Fig 3 (b) shows the sum along ray representation of the crack (the ray is oriented normal to the crack surface i.e. the crack has been tilted by 45 to obtain the representation). The crack has a very narrow opening in large regions which can also be seen in Fig 2 (c).
Additionally the maximum void volume fraction in the cubes ahead of the notch / crack can be seen in both Fig 3(a) and (b). It can clearly be identified that void growth has been substantially higher at crack initiation (higher than 4% void volume fraction ahead of the notch before coalescence) than in the slanted crack propagation regime where the void volume fraction has only reached levels around 1-2%. The change in fracture mechanisms between flat fracture initiation and slanted crack propagation can therefore clearly be observed and needs to be accounted for in modeling efforts.

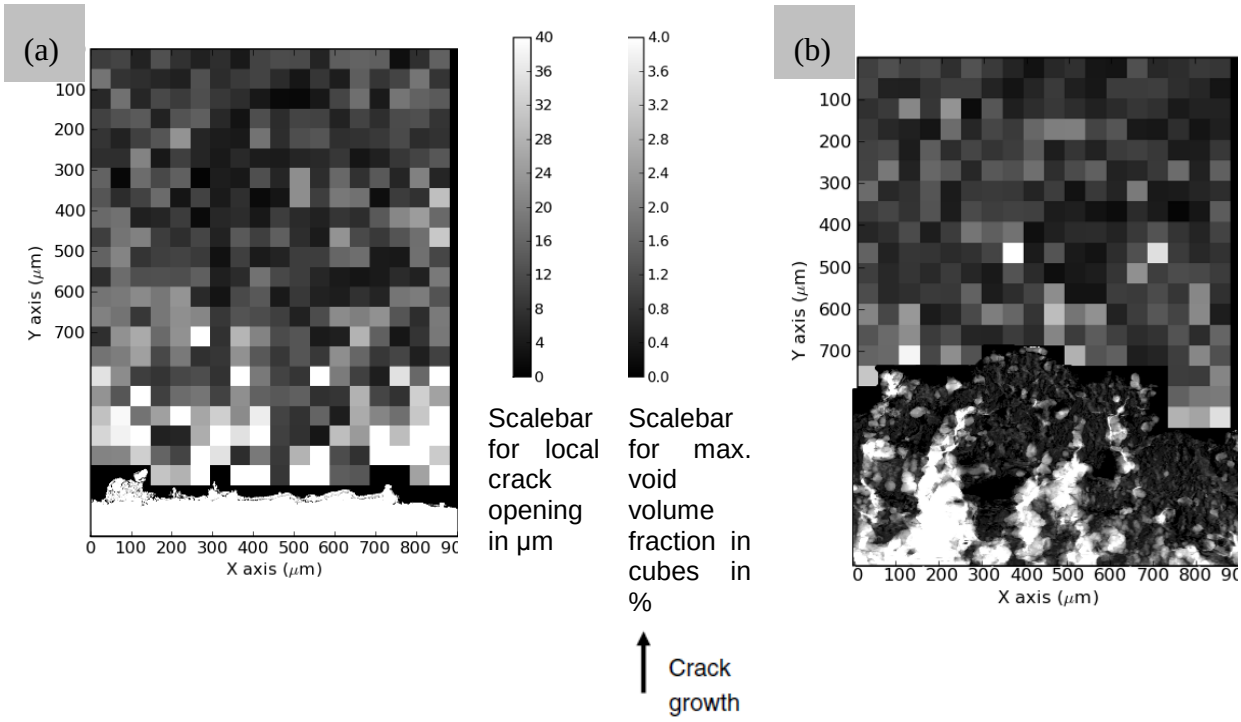

Fig. 3: 3D tomography analysis results of arrested cracks highlighting local crack opening and maximum void volume fraction in cubes ahead of the notch/ crack for test interruption in: (a) the initiation regime and (b) the slanted propagation regime (view normal to crack plane).

MODEL

In general terms, shear is thought to play a major role for the flat to slant transition and for ductile fracture. Thus a way is developed here to incorporate shear fracture in the Gurson

model framework. The idea is to add nucleation of a second population of voids as a function of the encountered stress state and, particularly shear. As shown in recent models [9, 10] the Lode parameter may be an adequate indicator for shear. Here the Lode parameter for strain rates, $\mu_{\dot{p}}$, is used based on the idea that it is the deformation rate in a shear configuration that may cause shear and slant fracture. $\mu_{\dot{p}}$ is defined as:

$$\mu_{\dot{p}} = \frac{\dot{p}_2}{\dot{p}_1 - \dot{p}_3} \text{ with } \dot{p}_1 \geq \dot{p}_2 \geq \dot{p}_3$$

Where $\dot{p}_i$ are the eigenvalues of the strain rate tensor. In the framework of the Gurson model the following equation for nucleation of a 2nd population of voids is generally used:

$$\dot{f}_n = A_n \dot{p}$$

Where $\dot{f}_n$ is the void nucleation rate, $\dot{p}$ the strain rate and A_n may be any positive function of the state variables.
It is suggested here to nucleate voids for a Lode parameter value close to μ = 0 (corresponding to generalized shear). A similar idea has been suggested in [10] where coalescence is suggested to occur at shear fracture. However, this model has not been applied to structures.
A very narrow Gaussian function around μ = 0 is used to obtain a continuous function. It is also suggested to nucleate from a certain critical strain p_c onwards. The following equation shows the suggested nucleation function:

$$A_n = A_0 e^{-\left(\frac{\mu_{\dot{p}}}{\mu_{\dot{p}}^0}\right)^2} \quad (p > p_c)$$

Where A_0 is a constant and $\mu_{\dot{p}}^0$ is a constant to adjust the shape of the Gaussian function.

SIMULATION RESULTS AND DISCUSSION

Here an example of a simulated flat to slant transition is presented. The model parameters are given in Table 2. Compared to the model presented in [6] kinematic hardening, plastic anisotropy and anisotropic void growth are neglected. The elastic-plastic behaviour has been identified on a tensile test in T direction. The following equation is used for isotropic hardening:

$$R(p) = R_0\left[1 + K_0 p + K_1(1 - e^{-k_1 p}) + K_2(1 - e^{-k_2 p})\right]$$

q1 and q2 are the GTN fitting parameters [14, 15] and f_0 is the initial void volume fraction.

Void growth		Damage		Nucleation for shear			
q_1	q_2	f_0		A_0	$\mu_{\dot{p}}^0$	p_c	
1.97	0.91	0.33%		2.0	0.011	0.1	
Elastic-plastic behaviour							
E in GPa	*v*	R_0 in *MPa*	K_0	K_1	k_1	K_2	k_2
70	0.3	250	0.0544	1.12	7.148	0.273	187.9
a=*b*=12							
Element sizes							
x=50 µm	y= 53 µm	z= 100 µm (through -thickness)					

Table 2 :Parameters for presented slant fracture simulation

The crack path found in the simulation is shown in Fig 4. The cracked elements are shown in orange. The flat triangular region close to the notch is clearly formed. It subsequently turns into a slant crack, consistent with experimental observations.

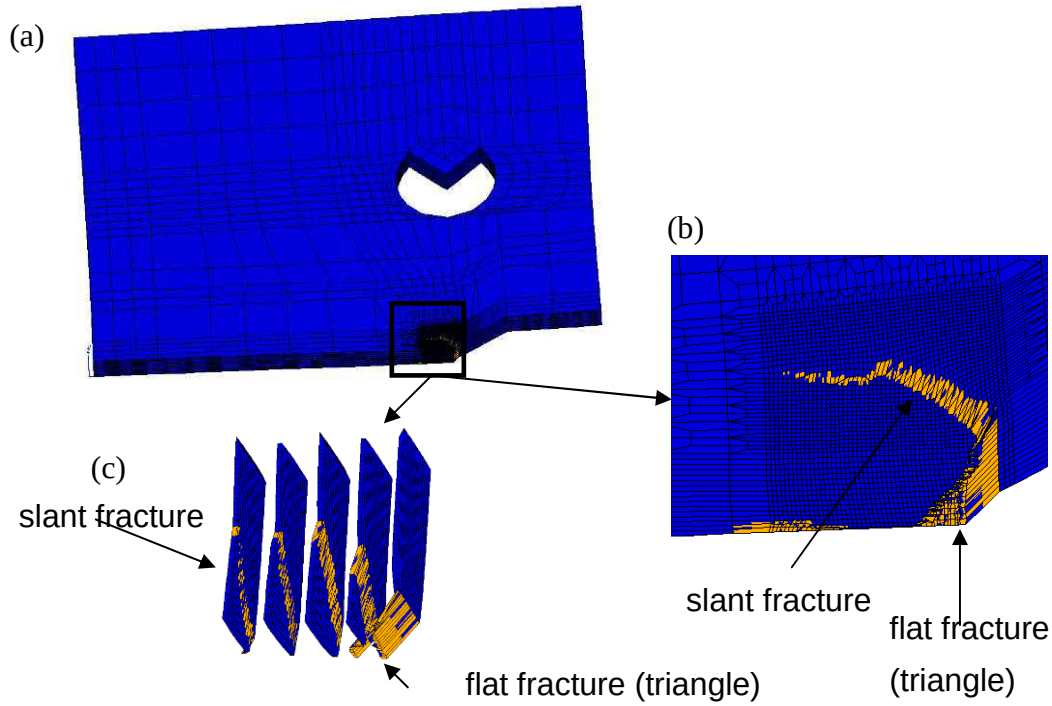

Fig. 4: Slant fracture simulation result:(a) meshed quarter of a Kahn tear test sample (b) zoom into finely meshed initiation region (c) element “slices” in the fine region. Broken Gauss points are shown in orange

Fig 5. shows the structural response in terms of Force F divided by initial ligament area A0 versus CMOD for experiments in T-L and L-T configuration and simulation results for T-L loading. The loads up to maximum load are predicted correctly. However, the load decrease in the simulation starts at a higher COD than in the experiment, so that the simulation results for the T-L configuration are located between the experimental results for T-L and L-T loading. The descending slope is however predicted correctly. Simulated loads are in the range of the experimental results which represents an advantage compared to other

attempts made to model slant fracture (e.g. [9, 7]) that did not fit experimental results or that were not compared to them.

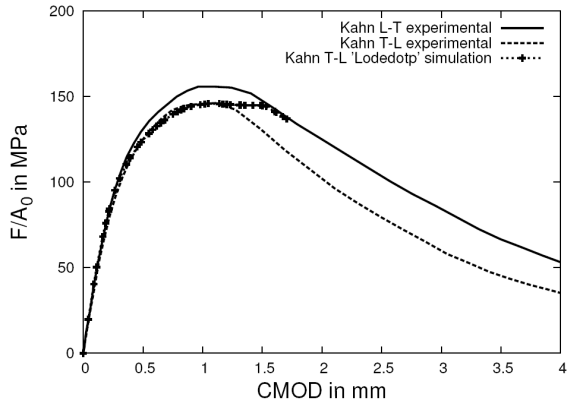

Fig. 5: Kahn tear tests: experimental and simulated structural response

These results show that accounting for shear fracture processes may lead to a better comprehension and prediction of slant fracture, the flat to slant transition and ductile fracture in general. The strong points of the model modification presented here are that predicted loads are in a reasonable range compared to simulations. The modification can easily be implemented in a Gurson model. Negative points are that 3 new parameters $\mu_{\dot{p}}^{0}$, A_0 and p_c need to be fitted which may be time consuming as computation times are long. A fine mesh needs to be used to be able to approximate the slanted fracture path. With progress in simulation techniques such as parallel computing, remeshing and non-local modeling these limitations may be overcome and the presented model may be used more easily for further shear fracture comprehension.

ACKNOWLEDGEMENTS

The authors acknowledge Alcan CRV for material supply. Ian Sinclair, Marco Starink, Frederic Bron and Bernard Bes are thanked for technical discussion. The authors also thank Elodie Boller at ESRF ID19 for support in micro-computed tomography.

REFERENCES

[1] Bron, F., Besson,J. Simulation of the ductile tearing for two grades of 2024 aluminum alloy thin sheets.
Eng Fract Mech, 2006. 73: 1531-1552.

[2] Garrison WM, Moody NR,
Ductile Fracture
J. Phys. Chem. Solids ,1987;48: 1035-1074

[3] Bron, F., Besson, J., Pineau,A.
Ductile rupture in thin sheets of two grades of 2024 aluminum alloy.
Mat Sci Eng A; 2004. 380: 356-364.

[4] Mahgoub E, Deng X, Sutton MA.
Three-dimensional stress and deformation fields around flat and slant cracks under remote Mode I loading conditions
Engng Fract Mech. 2003;70:2527-2542

[5] Morgeneyer TF, Starink MJ, Wang SC, Sinclair I,
Quench sensitivity of toughness in an Al alloy: Direct observation and analysis of failure at the precipitate-free zone
Acta Mater 2008;56:2872-2884

[6] Morgeneyer TF, Besson J, Proudhon H, Starink MJ, Sinclair I,
Experimental and numerical analysis of toughness anisotropy in AA2139 Al-alloy sheet
Acta Mater 2009;57: 3902-3915
[7] Besson J, Steglich D, Brocks WB.
Modeling of crack growth in sheet metal
Int J Solids Structures 2001;38:8259-8284
[8] Xue L. J.
Damage accumulation and fracture initiation in uncracked ductile solids subject to triaxial loading
Int. J. Solids Struct 2007 ;44 :5163-5181
[9] Xue L, Wierzbicki T.
Ductile fracture initiation and propagation modeling using damage plasticity theory
Eng Fract Mech 2008;75:3276-3293
[10] Nahshon K, Hutchinson JW.
Modification of the Gurson model for shear failure
Eur. J. Mech. 2008;27A:1-17
[11] Morgeneyer TF, Starink MJ, Sinclair I,
Evolution of voids during ductile crack propagation in an aluminium sheet toughness test studied by synchrotron radiation computed tomography
Acta Mater 2008;56: 1671-1679
[12] Kocsis M, Snirgirev A.
Imaging using synchrotron radiation
Nucl Instrum Methods Phys Res Sect A 2004;525A:79-84
[13] Toda H, Sinclair I, Buffière J-Y *et al*.
Assessment of the fatigue crack closure phenomenon in damage-tolerant aluminium alloy by in-situ high-resolution synchrotron X-ray microtomography
Philos Mag 2003;83:2429-2448
[14] Gurson AL. J.
Continuum theory of ductile rupture by void nucleation and growth: Part I- Yield criteria and flow rules for porous ductile media
Eng Mater Technol 1977;99:2-15
[15] Tvergaard V, Needleman
Analysis of the cup--cone fracture in a round tensile bar
A. Acta Metall 1984;32:157-169

.